Materials Science for Energy Technologies 3 (2020) 611–625

Contents lists available at ScienceDirect

Materials Science for Energy Technologies

journal homepage: www.keaipublishing.com/en/journals/materials-science-for-energy-technologies

Utilization of phosphogypsum in CO_2 mineral sequestration by producing potassium sulphate and calcium carbonate

Adil Lachehab [a], Oumaima Mertah [b], Abdelhak Kherbeche [b], Hicham Hassoune [a,*]

[a] Department of Chemical and Biochemical Sciences (CBS), Mohammed VI University Polytechnic, Morocco
[b] Laboratory of Catalysis, Materials and Environment (LCME), Sidi Mohamed Ben Abdellah University, Fez, Morocco

ARTICLE INFO

Article history:
Received 5 April 2020
Revised 17 June 2020
Accepted 19 June 2020
Available online 5 July 2020

Keywords:
Potassium sulphate
Phosphogypsum
CO_2 sequestration
Mineral carbonation
Calcium carbonate

ABSTRACT

Industrial activities for the phosphoric acid production cogenerate a large amount of phosphogypsum waste, emitting significant quantities of toxic gas in the surrounding environment. In the context of recovered materials to handle greenhouse gases more precisely CO_2 as one of the most toxic gases responsible for the global climate change, an affordable and effective method for CO_2 mineral sequestration using phosphogypsum by-product is developed in this investigation. The obtained results show the high efficiency of portlandite $Ca(OH)_2$ resulting from the dispersion of phosphogypsum in alkaline potash solution followed by releasing of potassium sulphate as a co-product. Furthermore, the carbonation experiments show a total conversion of the $Ca(OH)_2$ to calcium carbonate as final product at ambient temperature and atmospheric pressure. The approach suggested in this research shows permanent and safe solution to face the storage of phosphogypsum and carbon dioxide, which were causes a serious problems for the ecosystems and human health. As well as, the valorization of the co-products in different fields, e.g., potassium sulphate as a fertilizer while calcium carbonate has various uses as raw material for construction.

1. Introduction

The world is at a critical stage in its efforts to fight against climate change. The Intergovernmental Panel on Climate Change (IPCC) have released a report explain the telling increase in carbon dioxide concentrations in the atmosphere due to constantly increasing of anthropogenic greenhouse gas emissions, which has been the main factor to the rising in global temperatures in recent years. The IPCC concluded that, in the absence of fully committed and urgent action, climate change would have severe and irreversible impacts across the world [1]. Compared to other greenhouse gases, CO_2 is the most important one considered as responsible for about 64% of the enhanced greenhouse effects [2]. Fossil fuels are the dominant form of energy utilized in the world (86%), and account for about 75% of current anthropogenic CO_2 emissions [3]. If recent trends in global CO_2 emissions continue, the world will not be on a path towards stabilization of greenhouse gas concentrations [1]. From the energy sector, global CO_2 emissions are around 30 billion tons per year, it is expected that this number will be doubled by 2050 [4]. For this reason, It has been estimated that there is necessary to stabilize CO_2 levels in the atmosphere, by reducing CO_2 levels up to 85% over the next century this impose a reduction of around 20 billion tons of CO_2 each year [4–6]. Therefore, this estimation requires to adopt a common ultimate objective of reducing the emissions of CO_2 to control the global temperature rise [7–8]; all these studies lead to the necessity to find effective strategies for controlling global CO_2 levels.

The carbon capture and storage is a technically feasible method of making deep reductions in CO_2 emissions. Then, the CO_2 must be transported to a storage site where it will be stored away from the atmosphere for a very long time [1].

The most important technologies of large-scale for carbon capture and storage are as follows: ocean, where CO_2 directly injected into the ocean by moving ships, stationary points or by long bottom-mounted diffusers, however, they cannot be avoided the negative effects on marine ecosystems [9]. In geological sequestration where CO_2 stored below ground by injecting CO_2 into profound geological formations, which is requires a comprehensive geophysical investigations that need to be precisely achieved before geological sequestration [10,11]. As well as mineral carbonation, which is considered as the most promising permanent

* Corresponding author at: Department of Chemical and Biochemical Sciences, Mohammed VI Polytechnic University, B.P. 118, El Jadida, Morocco.
E-mail addresses: h.hassoune@ocpgroup.ma, hicham.hassoune@um6p.ma (H. Hassoune).

Peer review under responsibility of KeAi Communications Co., Ltd.

https://doi.org/10.1016/j.mset.2020.06.005

method [12,13]. This process has gained attention recently (Olajire, 2013) [14] as an effective process to sequester CO_2 into solid carbonates permanently and inherently safe storage due to the thermodynamically stable nature of the carbonate product formed [15,16]; Such as Magnesite $MgCO_3$ [17], and calcite $CaCO_3$ [18]; in fact, the energy state of carbonates are 160–180 kJ/mol lower than the energy state of CO_2 400 kJ/mol [19]. The most natural minerals containing enormous amount of major cations Ca^{2+} and Mg^{2+} are olivine [20], serpentine [21], wollastonite [18], and tremolite [22]. As well as certain industrial wastes, such as blast furnace slag [23], waste cement [24] and waste gypsum [19], which have been used as raw materials for CO_2 carbonation.

Phosphogypsum is an important by-product resulting from the production of phosphoric acid by "wet acid method" and usually takes the form of calcium sulfate dehydrate $CaSO_4{\cdot}2H_2O$ [25]. It contains also impurities such phosphoric acid, fluoride, trace metals (Cr, Cu, Cd and Zn) and radioactive elements (U, and Th), as well as rare earth elements [26]. This material occurs as a waste in the fabrication of phosphoric acid from calcium phosphate ore $Ca_{10}(PO_4)_6F_2$ and sulfuric acid (Eq. (1)). Untreated phosphogypsum is naturally acidic caused by the residual phosphoric acid, sulphuric acid and also hydrofluoric acid inside the porous structure. The ratio of the composition of phosphogypsum is depends on the origin and to the process of phosphoric acid production from phosphate rock, but the composition is basically unaltered [27]. The chemical reaction for dehydrate process is:

$$Ca_{10}(PO_4)_6F_2 + 10\,H_2SO_4 + 20\,H_2O \rightarrow 10\,CaSO_4.2\,H_2O + 6\,H_3PO_4 + 2\,HF \quad (1)$$

The sulphuric acid process is considered as economic; nevertheless, it manufacture large quantities of waste, illustrated by the global production of phosphogypsum approximately 100–280 Mt per year all over the world [28]. During phosphoric acid production, a large amount of phosphogypsum produced which surpass the mass of the final product, about 5 tons of phosphogypsum is generated per ton of phosphoric acid manufactured [29]. However, this enormous amount of phosphogypsum produced is disposed without any treatment; is mainly dumped directly at the sea [25] or, stockpiled in the vicinity of the factory [30], this latter remains the most practice applied. According to the literature, 15% of world phosphogypsum production is recycled. Such as in soil remediation [31], cement production [32], filler in papermaking [33], as a new fire-insulating material [34]; and in the production of chemical raw materials (such as calcium chloride, ammonium sulphate, sodium sulphate, thiourea, sodium hydrogen phosphate, etc.) [27,29]. The remaining 85% is disposed of without any treatment [29]. However, prospective processes for large-scale utilization of phosphogypsum are still under investigation. This industrial by-product is a problem in several countries of the world such as Morocco, Tunisia, South Africa, China and Florida [35]. It has a value which is not enough exploited. In fact, its high content of calcium and sulfur makes it a valuable waste, and its valorization could be economical and, at the same time, to solve an environmental problem. Previous studies have been conducted on environmentally applications of phosphogypsum, especially for CO_2 sequestration and they have assured that phosphogypsum can be a very suitable feedstock for mineral carbonation with a view to reduce the greenhouse gases emissions [27,35–38].

The proposal discussed in this work is to evaluate the use of by-product phosphogypsum because of the enormous amounts produced annually, as a calcium Ca source for carbon dioxide mineral sequestration; by conversion of phosphogypsum into an agent calcium hydroxide $Ca(OH)_2$ for carbon sequestration and potassium sulphate by alkaline dissolution with caustic potash to produce potassium sulphate K_2SO_4 [39].

2. Materials and methods

2.1. Materials

The samples used in this study were collected from the rotatory separation filter of phosphogypsum present in the phosphoric acid unit, El Jadida Morocco. Potassium hydroxide (KOH), CO_2 gas with high purity (>99.9%) used in this research were purchased from Solvachim, Flosit in Morocco, respectively. While, commercial grade calcium carbonate ($CaCO_3$), potassium sulphate (K_2SO_4) and pure gypsum were purchased from Solvachim in Morocco, Prolabo in France, respectively and were used for comparison studies.

2.2. Sample preparation

The samples used in this study were collected from the rotatory separation filter of Phosphogypsum present in the phosphoric acid unit, El Jadida Morocco. Phosphogypsum is considered as a by-product in the phosphoric acid production. It contains soluble and insoluble impurities that must be removed. Some of these impurities may be removed by simple means, e.g., washing with water, while others may need complex methods of treatment that tend to be costly [40]. In the first step, phosphogypsum sample was washed several times until the purity of the sample, and neutral pH, then oven-dried at 60 °C until complete dryness, ground and homogenized.

In the next step, the process starts by the dispersion of the raw sample in an alkaline solution. 10 g of phosphogypsum was dispersed in 70 mL of distilled water by magnetic stirring at room temperature. Subsequently, 6.51 g of KOH was added to reach an OH^-/Ca molar ratio of 2. The mixture was magnetically stirred at room temperature for 3 h.

Finally, the dispersion of the phosphogypsum sample leads to the formation of two phases

Eq. (2): whitish solid phase and a liquid phase. After filtration of the solution, the resulting liquid was evaporated on a hot plate at 80 °C, and solid phase was oven-dried at 60 °C.

$$CaSO_4 \cdot 2\,H_2O + 2\,KOH \rightarrow Ca(OH)_2 + K_2SO_4 + 2\,H_2O \quad (2)$$

2.3. Characterization

The physical and chemical characteristics of the phosphogypsum and the solid products were investigated using X-ray diffraction characterizations, which were performed on a Bruker diffractometer (XRD; X'PERT PANALATYCAL) using Cu-Kα radiation (λ = 0.154060 nm) with the scanning speed of 1° per minute in the interval $5° < 2\theta < 70°$; operated at 40 KV and 30 mA to identify the crystalline phases of the samples. X-ray fluorescence (XRF; OXFORDMDX1000) to determine the major elements and compounds of the products.

The inductively coupled plasma mass-spectrometry (ICP-MS; Thermo Jarrell ash iris) to identify the trace elements. Scanning Electron Microscopy coupled with an energy dispersive spot (SEM-EDS; FEI QUANTA 200) was used to show the surface morphology and the compositions of the products. Fourier Transform Infrared Spectroscopy (FTIR; Jasco spectrum FTIR-4100 type A) was performed for chemical bond determination in the mid-infrared region from 400 cm^{-1} to 4000 cm^{-1} under ambient air condition using KBr as a diluent. And TG-DTA analyses was carried out in Thermogravimetric– Differential Thermal analyzer (TGA-60H Shimadzu) under a nitrogen atmosphere at a heating rate of 10 °C/min from 25 °C to 1000 °C, it was used to determine the weight loss of CO_2.

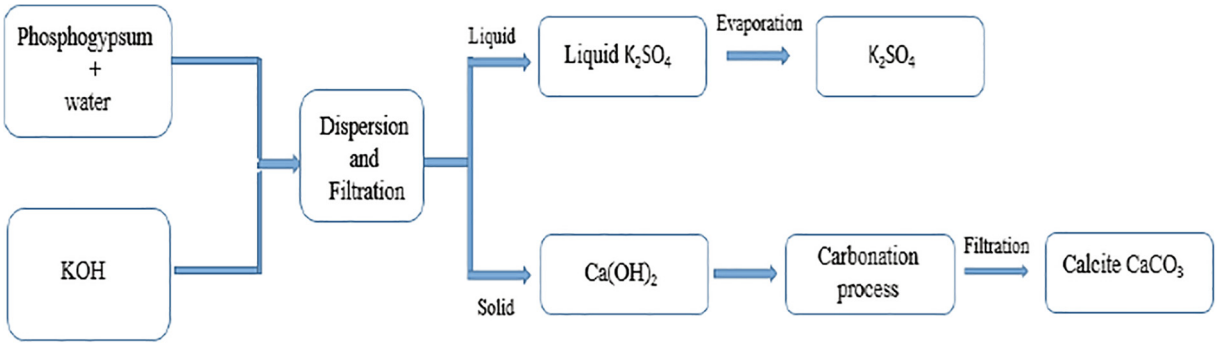

Fig. 1. General scheme of the experimental procedure.

2.4. Synthesis of $CaCO_3$ during the carbonation experiments

Phosphogypsum carbonation was conducted in a 150 mL mini reactor assembly (three-necked glass reactor vessel) at room temperature and atmospheric pressure. At the beginning of the experiment, 2 g of the solid phase dried was dispersed in 40 mL of distilled water under magnetic stirring. After 5 min, CO_2 gas (1 bar, 1.2 $L.s^{-1}$) was continuously injected into the reactor until stabilization of the pH approximately 7.0, the reaction was stopped. In this reaction, the solution rich in Ca reacted with CO_2 to form $CaCO_3$ as in Eq. (3). Afterwards, the carbonation solution was filtered, the recovered precipitates were oven-dried at 60 °C, and the supernatant was discarded (Fig. 1). The experimental methods used in this work are summarized in Fig. 1.

$$Ca(OH)_2 + CO_2 \rightarrow CaCO_3 + H_2O \quad (3)$$

Finally, the carbonation product dried was analyzed to identify the composition of the products. Considering that phosphogypsum contains important amount of Ca, for this reason, we expected the possibility of producing calcium carbonate $CaCO_3$ with high purity in the carbonation process.

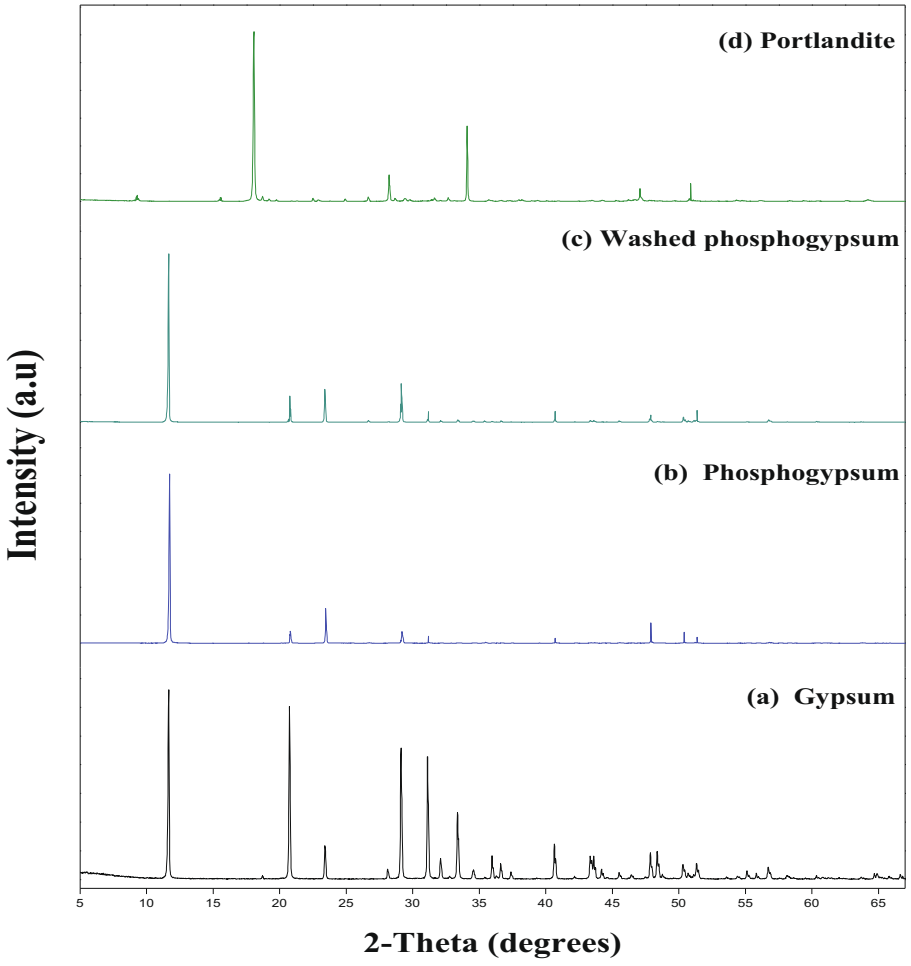

Fig. 2. XRD analysis of (a) the commercial gypsum, (b) the phosphogypsum ($CaSO_4{\cdot}2H_2O$), (c) washed phosphogypsum and (d) portlandite.

3. Results and discussion

3.1. Chemical properties

The main mineral phase of the raw phosphogypsum was characterized by X-ray diffraction analysis. As shown in Fig. 2b, the XRD results confirmed that the mainly composed of phosphogypsum is calcium sulfate $CaSO_4{\cdot}2H_2O$ The major peaks of $CaSO_4$ was identified at 11.71°, 20.80°, 23.44° and 29.16°, while some minor peaks was observed at 31.16°, 40.69°, 47.86°, 50.37° and 51.35. This result correlate suitably with previous research and commercial gypsum [27,36]. In order to achieve an interest purification of phosphogypsum, it was washed several times to eliminate some impurities before being used and was characterized by XRD. As displayed in Fig. 2c there is no difference between phosphogypsum brut and washed, it still keeping the composition of this by-product and maybe the modification will be confirmed by the XRF and ICP analysis.

The XRD pattern of the solid phase obtained after dispersion of phosphogypsum by addition of KOH illustrate that is correspond principally to portlandite $Ca(OH)_2$ as supposed by Eq. (2). As observed in the Fig. 2d, the peaks correspond to portlandite were detected at 18.03°, 28.64°, 34.05°, 47.06°, 50.89° [37], which confirms that portlandite was well synthesized, while the liquid phase was evaporated to obtain a transparent salts precipitated which is mostly constituted of potassium sulphate K_2SO_4. The XRD patterns (Fig. 3a and b) are illustrated the synthetic and commercial K_2SO_4 for comparison. The pattern of the synthetic K_2SO_4 sample could be well matched to the XRD peaks of pure orthorhombic K_2SO_4 as shown in Fig. 3a. The representative peaks observed at 21.25°, 30.77°, 40.45° and 51.47° were the orthorhombic structure of K_2SO_4, which is consistent with the previous studies [38]. In this context, the result of XRD for the co-product coming from the dispersion of phosphogypsum with KOH base is as expected, according to Eq. (2). The only crystalline phase detected was arcanite, which correspond the more stable phase mineral.

The constituents of raw phosphogypsum were analyzed using X-ray fluorescence analysis in order to determine the main species and impurities in phosphogypsum. The major compositions of phosphogypsum are shown in Table 1, it has varies according to the type of wet phosphoric acid process used [25]. The XRF result shows that the phosphogypsum is clearly composed by CaO (27.079%), SO_3 (29.335%), as well as a small amount of SiO_2 (0.586%) and some minor impurities depend on the source of the phosphate rock as shown in Table 2 such as SrO, Y_2O_3, and others, not observable by XRD. As we can observe, by washing phosphogypsum, the amounts of impurities was decreased and this is a benefit for producing purified products in the next step. Again, the phosphogypsum is rich in Ca, which is makes it favorable and a potential minerals for CO_2 sequestration to form stable carbonate.

Portlandite $Ca(OH)_2$ is principally dominated by CaO (38,147%), as shown in the Table 1, the amount of calcium remains higher comparing with the other compositions which appear on the form of impurities transformed from raw phosphogypsum. As well, the High CaO content involve a good synthesis of the portlandite for the production of calcium carbonate through mineral carbonation.

In order to identify trace elements presented and to know the environmental consequences that these samples under study may produce, it is required to analyze by inductively coupled plasma emission spectrometer ICP-MS (Table 3) and compared to the global concentration of trace elements for a typical soil [41,42]. According to Table 3, the main trace elements detected in phosphogypsum were Cd, Cr, Ni, V and Zn. The amounts of these trace elements in the products from phosphogypsum dispersion

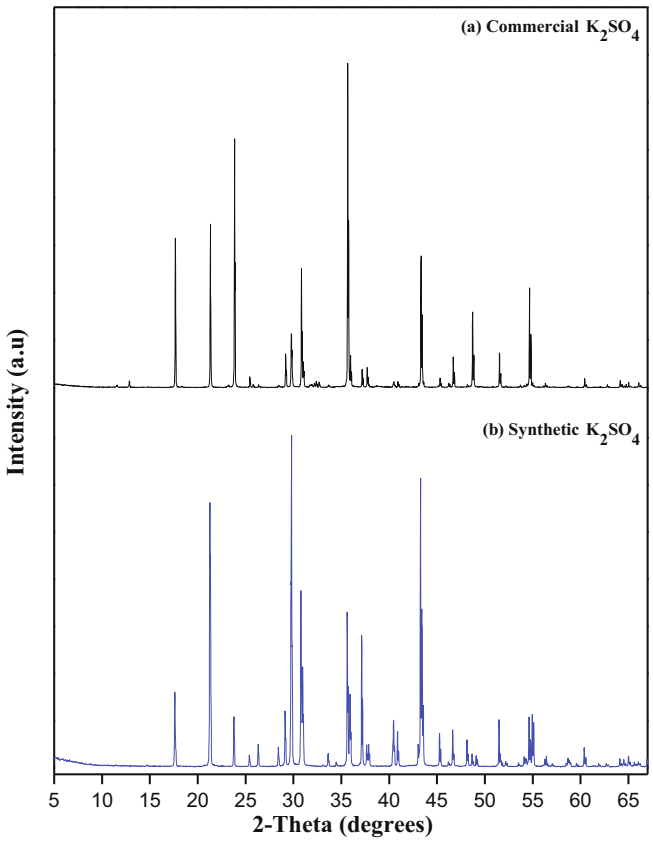

Fig. 3. XRD analysis of (a) the commercial, and (b) the synthetic potassium sulphate K_2SO_4.

including portlandite, sulphate potassium and calcium carbonate, adding the commercial $CaCO_3$ and K_2SO_4 for comparison, are also displayed in Table 3. It can be concluded that all trace elements were occur at value $\leq$ 14.1 ppm that is below the concentration of a typical soil and the amounts of these elements are inferior than those occurred from other sources of phosphate rock in the world [29,42]. Generally, there was a decrease in content of trace elements in phosphogypsum compared with the obtained products and the most contents of those are transferred from phosphogypsum to the portlandite produced.

Therefore, only a very few contents were remained in the potassium sulphate ensue from the phosphogypsum dispersion. For example, Cr content in the raw phosphogypsum was about 5.4 ppm compared to <1 ppm in potassium sulphate synthetic; as a result, its effect can be excluded and this means that the co-products can be used as raw material in different applications without causing any environmental effects. In addition, these values are approximately to those found in the literature [43] and to the commercial one.

Table 1 summarized the main constituents of the synthetic and the commercial K_2SO_4. As shown in this table, the constituents dominates in the potassium sulphate are K_2O (24.96%) and SO_3 (15.77%), also containing CaO (6.65%) jointly with some insignificant impurities.

However, the calcium oxide compound is transferred to K_2SO_4 in the form of impurities, in addition to other elements with low contents such as: SrO, Fe_2O_3, MgO, etc. (Table 2). As expected, these elements are appeared from raw phosphogypsum, which confirm their absence in the pure K_2SO_4. These results are in accordance with the XRD patterns and as expected by Eq. (2).

Table 1
Major elements contents (wt%) of the samples analyzed by X-ray fluorescence.

Elements	Phosphogypsum		Gypsum	Portlandite	Potassium sulphate		Calcium carbonate	
	Brut	washed	commercial		synthetic	commercial	synthetic	commercial
Constituent (wt%)								
CaO	27.079	34.132	31.584	38.147	n.d.	n.d.	53.740	63.343
K_2O	n.d.	n.d.	n.d.	16.209	33.475	44.126	2.955	n.d.
SO_3	29.335	42.163	38.061	23.654	14.315	35.532	15.366	n.d.
P_2O_5	0.715	n.d.	n.d.	0.793	0.207	0.177	n.d.	n.d.
SiO_2	0.586	0.481	0.127	0.598	0.749	0.802	0.235	0.780
Al_2O_3	0.345	0.642	0.371	n.d.	n.d.	n.d.	n.d.	0.386

n.d., not detected.

Table 2
Trace elements contents (ppm) of the samples analyzed by X-ray fluorescence.

Elements	Phosphogypsum		Gypsum	Portlandite	Potassium sulphate		Calcium carbonate	
	Brut	washed	commercial		synthetic	commercial	synthetic	commercial
Trace elements (ppm)								
MgO	382.9	n.d.	n.d.	115.1	62.7	0.159	n.d.	0.159[a]
TiO_2	199.8	168.8	n.d.	137.4	121.2	255.6	62.6	n.d.
V_2O_5	0.0	n.d.	16.5	n.d.	n.d.	22.6	15.7	n.d.
Fe_2O_3	121.2	n.d.	118.6	204.5	158.8	0.125[a]	247.0	211.3
SrO	650.9	805.7	0.164[a]	684.9	775.6	116.4	18.2	n.d.
Y_2O_3	144.3	129.7	n.d.	113.3	136.8	n.d.	136.8	n.d.
ZrO_2	3.1	4.9	3.6	7.1	0.0	3.9	n.d.	n.d.
Nd_2O_3	58.7	63.1	n.d.	19.1	n.d.	n.d.	12.6	n.d.
Yb_2O_3	0.0	0.0	5.9	0.0	n.d.	n.d.	n.d.	n.d.
SnO_2	n.d.	n.d.	110.1	n.d.	n.d.	181.3	n.d.	n.d
Co_3O_4	n.d.	n.d.	n.d.	41.7	n.d.	n.d.	7.4	n.d.
Lu_2O3	n.d.	n.d.	n.d.	n.d.	n.d.	15.4	n.d.	9.2

[a] : weight percent (wt%).

Table 3
Contents (ppm) of some trace elements in the samples measured by analysis with ICP-MS.

Elements	Phosphogypsum		Portlandite	Potassium sulphate		Calcium carbonate	
	Brut	washed		synthetic	commercial	synthetic	commercial
Trace elements (ppm)							
Cr	5.1	<2	3.4	9.2	14.1	3.2	4.0
Ni	2.9	<2	<2	2.0	2.3	<2	2.1
V	4.7	3.6	3.5	<3	<2	<3	10.3
Cd	5.4	1.2	1.3	<1	<1	1.5	1.5
Zn	4.2	3.4	3.7	<3	<2	5.5	10.6

In addition, the structure of phosphogypsum has been confirmed by using a FTIR spectrophotometer at the wavelength ranged from 400 cm^{-1} to 4000 cm^{-1}. The FTIR spectrum of phosphogypsum, displayed in Fig. 4a, shows that the bands occurs at 662.43 cm^{-1} and 594.35 cm^{-1} are assigned to the stretching and bending modes vibration of sulfate [44]. Moreover, the characteristic bands observed at 3352.90 cm^{-1} and 1626.12 cm^{-1} correspond to the stretching and bending vibration of O—H in water molecules [45]. The band situated at 1147.83 cm^{-1} is assigned to O—S—O stretching vibration of SO_4^{2-} [46]. These bands are very close to the published data in the literature [47].

The FTIR spectrum of portlandite $Ca(OH)_2$ as synthesized is presented in Fig. 4b. The O—H stretching vibration band observed at 3640.07 cm^{-1} corresponding to the calcium hydroxide [48]. The bands observed at 3411.33 cm^{-1} and 1675.71 cm^{-1} are assigned to stretching and deformation vibration mode of chemisorbed water [45]. In addition, the absorption bands at 1495–1413 cm^{-1} and 871.89 cm^{-1} are assigned to different vibration mode C—O of carbonate groups CO_3^{2-} [45,49], also the presence of a small band at 2107.62 cm^{-1} is due to stretching mode of C—O present in the sample which indicates the contamination of sample by CO_2 in the atmosphere. The observed band at 2509.81 cm^{-1} in the spectra is attributed to water-water interaction [50], while the Si—H stretching vibration band is observed at 2267.58 cm^{-1} [51].

The FTIR spectrums of synthetic and commercial potassium sulphate are displayed in Fig. 5. The band observed at 3439.49 cm^{-1} is corresponding to the asymmetric O—H stretching vibration present in the compound Fig. 5b [45,52]. The band observed at 1435.31 cm^{-1} corresponds to the presence of COO^- in the K_2SO_4. The FTIR spectrum of SO_4^{2-} ion present in the compound has two absorption bands observed at 1103.07 cm^{-1}, and 619.74 cm^{-1}. The characteristic peaks obtained in this study correlates closely with previous studies [53] giving single strong band at 619.74 cm^{-1} assigned as asymmetric stretching vibration of S—O. Moreover, the spectra for potassium sulphate produced from the phosphogypsum was similar to the potassium sulphate from the commercial brand Fig. 5a, and resembles in the most region. As a result, the K_2SO_4 was well synthesized from the raw phosphogypsum.

3.2. Textural properties

The particle size distribution of the phosphogypsum was analyzed by a laser diffusion particle analyzer (Malvern PANalytical). The particle size analysis (Fig. 6) showed that the phosphogypsum

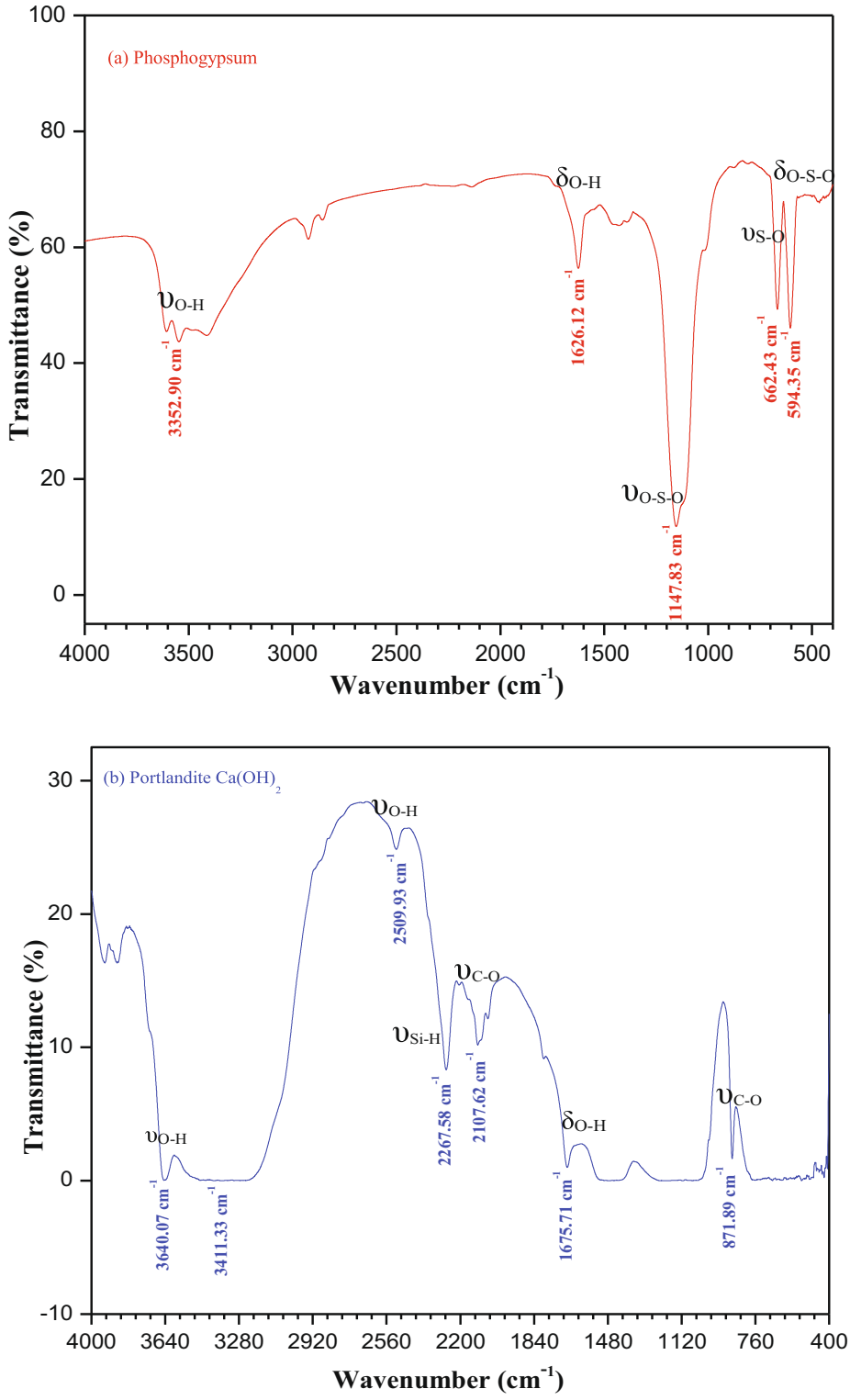

Fig. 4. FTIR analysis of (a) the phosphogypsum, (b) Portlandite $Ca(OH)_2$.

has grain size on the micrometric scale whose length is between 1 and 100 μm.

The Scanning Electron Microscopy analysis shows high relevant information on the morphology of the samples.

The SEM-EDS images of the phosphogypsum and washed phosphogypsum approved the XRD results and showed the existence of different solid phases, as observed in Fig. 7a–c. The phosphogypsum crystals observed are presented in different forms, in the form of tubular, in rhombic form, as well as small crystal clusters form. It can also be observed the presence of metals and some small particles, which is in good agreement with XRF analysis, see Table 1 and Table 2, and previous studies

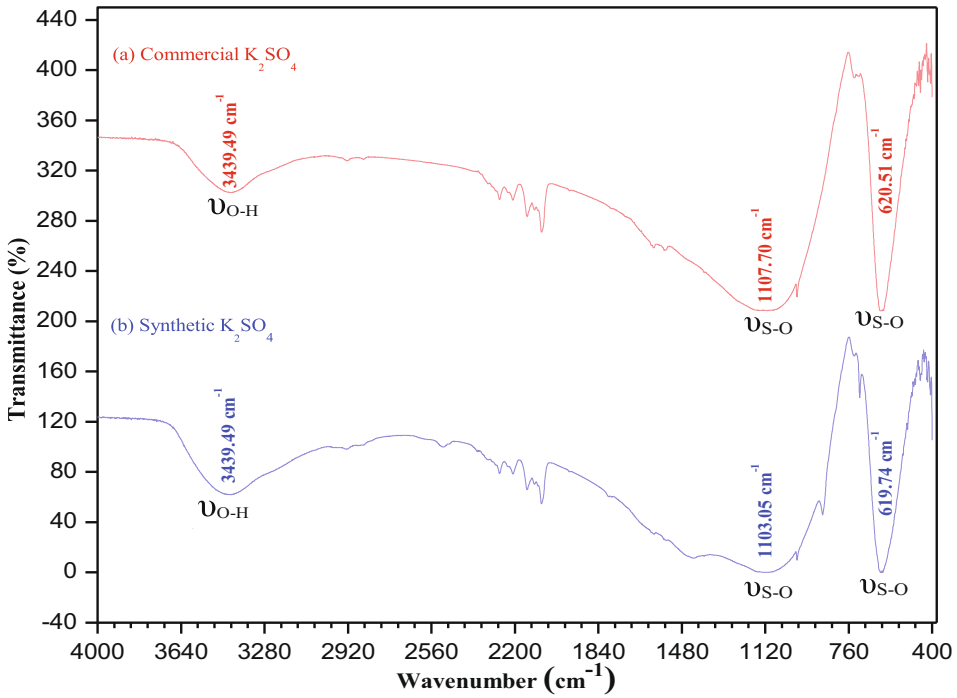

Fig. 5. FTIR analysis of (a) the commercial and (b) the synthetic potassium sulphate K_2SO_4.

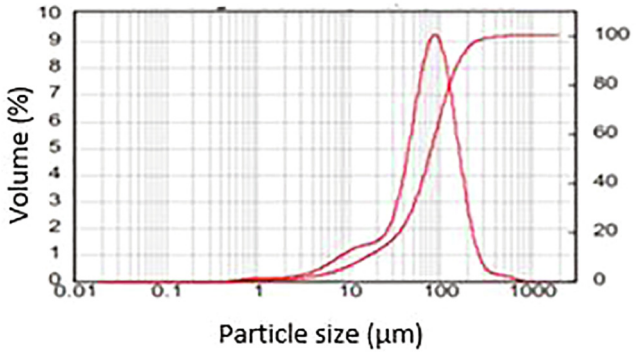

Fig. 6. Particle size distribution of phosphogypsum.

[54–56]. Moreover, the washed revealed more clearly, intense and assured the same forms.

In order to verify the chemical composition of the phosphogypsum, the EDS energy spectra of was used to analyze the elemental content. The results of EDS are shown in Fig. 6b–c and Tables 4, confirms the presence of Ca (38.91 wt%), F (35.00 wt%), O (14.89 wt%) and traces of Na, P, Al. It can be concluded that the main constituents of the substance is $CaSO_4$ similar to natural gypsum [57].

It is indicated in the literature that the most common structure of portlandite is hexagonal [62]. Fig. 8 represents the SEM-EDS analysis of the portlandite formed. As shown in this figure, the crystals obtained were clear, intense with similar size. Moreover, a perfectly hexagonal and regular structure of this product confirms the high purity of $Ca(OH)_2$ as the main product of the experiment by the dispersion of phosphogypsum in acoustic potash , as expected in Eq. (2) and confirmed by EDS in Fig. 8b and Table 4 (Ca (82.97 wt%), and O (24.70 wt%)).

A representative SEM-EDS images, corresponding to the synthetic and the commercial potassium sulphate, are shown in Fig. 9a and c. It can be observed that the particle present as a uniform orthorhombic crystals of different sizes (Fig. 9a), which is characteristic of potassium sulphate K_2SO_4 [58]. The surface chemical composition obtained by EDS analysis (Fig. 9c and Table 4) shows several well defined peaks for K (41.71 wt%), S (18.34 wt %), and O (22.20 wt%) which confirmed that the synthesized material is potassium sulphate, that is consistent with the XRF, XRD results and commercial K_2SO_4.

The by-product phosphogypsum was decomposed to SO_4^{2-} when it's disperse in caustic potash. Thus, SO_4^{2-} reacts directly with K^+ to form K_2SO_4. The main participant to potassium sulphate increase are the presence of KOH and $CaSO_4$. However, the existence of small grains revealed the presence of impurities as shown in the image and not appearing in the commercial K_2SO_4 (Fig. 9b) but confirmed by XRF and ICP-MS.

3.3. Carbonation efficiency

The XRD patterns in Fig. 10a represents the carbonation product resulting from the carbonation process comparing with commercial $CaCO_3$ (Fig. 10b). The representative peaks at 29.36°, 36.63°, 39.35°, 56.69°, and 57.35° are corresponding to Calcite, while, the peaks at 23.36°, 43.30°, and 48.39° are corresponding to Vaterite. As a result, the product resulted from the reaction between portlandite $Ca(OH)_2$ and CO_2 was obviously the calcium carbonate as presented in Eq. (3). This result is in agreement to other studies [36,42] and is similar to the $CaCO_3$ from the commercial brand. Moreover, the XRD pattern suggests that there are also small peaks corresponding to gypsum crystals, which signifies that some part of phosphogypsum keep it unreacted during the carbonation experiments.

Phosphogypsum showed high carbonation reactivity at room temperature and atmospheric pressure for CO_2 sequestration, producing calcium carbonate [11,36,54]. In order to investigate the efficiency of the carbonation process adapted in this study, the TG-DTA of the carbonate product was realized.

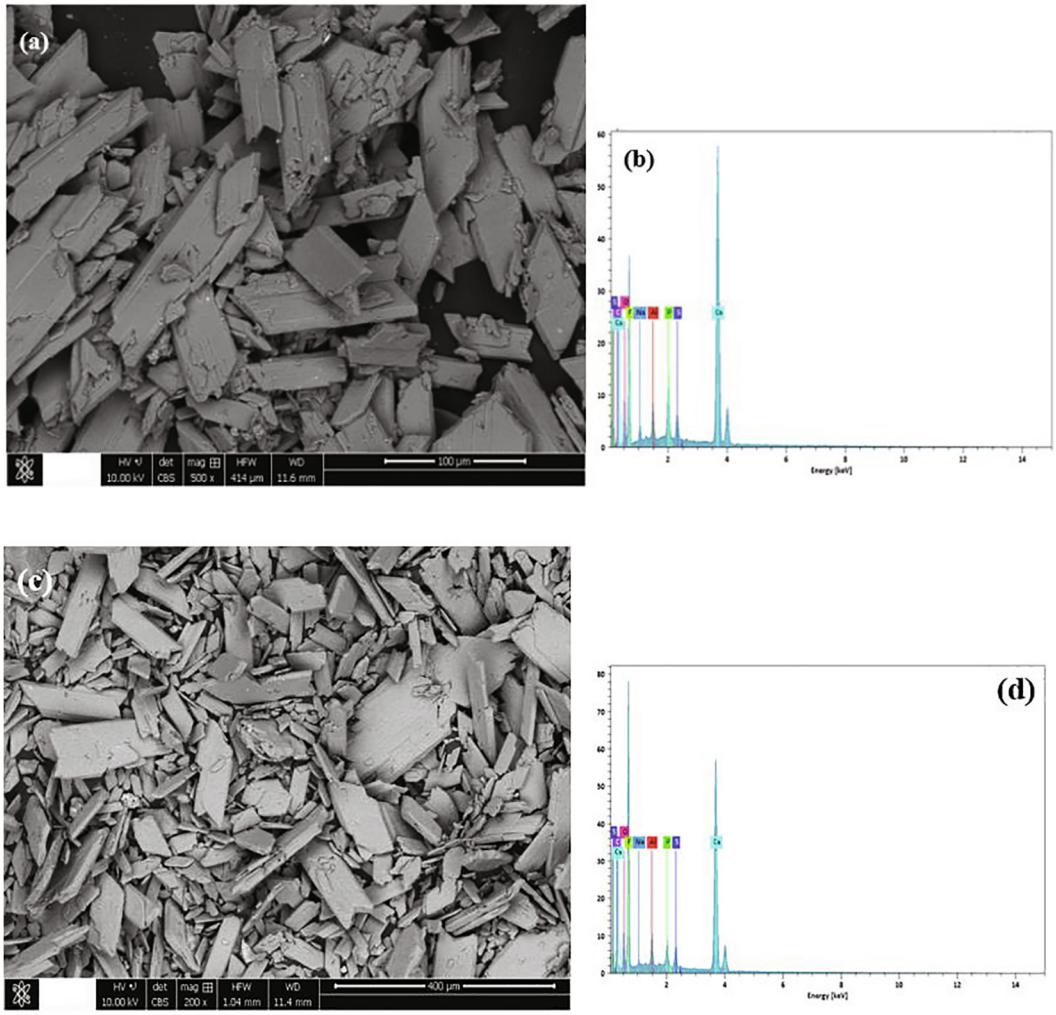

Fig. 7. SEM-EDS analysis of (a)-(b) the phosphogypsum, (c)-(d) washed phosphogypsum.

Table 4
Weight percent of the samples obtained by SEM-EDS.

Elements	Phosphogypsum		Portlandite	Potassium sulphate		Calcium carbonate	
	Brut	washed		synthetic	commercial	synthetic	commercial
Elements (wt%)							
O	14.89	14.29	24.70	22.20	5.48	65.29	28.57
C	2.89	8.90	0.84	1.50	–	14.54	5.97
Ca	38.91	37.05	82.97	–	–	41.26	47.08
S	1.69	1.69	3.33	18.34	20.08	0.65	–
K	–	–	2.80	41.71	52.34	–	–
F	35.00	59.89	–	–	–	–	–
Na	1.56	0.99	–	–	–	–	–
P	1.62	2.01	–	–	–	–	–
Al	2.21	2.48	–	–	–	–	–

Thermal behavior of carbonation product is of wholly importance to be understood. The TG-DTA curves of thermally treated product of the carbonation experiments are shown in Fig. 11a. According to the results of XRD and XRF, they are composed mainly of calcium carbonate. The TGA curve shows an important endothermic peak in the range of 550–800 °C, and that was likely due to the decomposition of calcium carbonate formed in the carbonation process to liberate CO_2 gas. As expected in Eq. (4) with the weight loss of 31.98% [42,59].

$$CO_3 \rightarrow CaO + CO_2 \quad (4)$$

The most significant DTA peak takes place at 682.1 °C during heating of the calcium carbonate at temperatures from 650 to 800 °C. At this range, the most weight loss is owing to evaporation of sulphate phases [19].

A second weight loss between the temperatures of 100–150 °C indicated that the dehydration was taken place at 109.65 °C. Based on a previous study of similar product $CaCO_3$ [19,36–37] and from TG-DTA curves, it can be concluded that

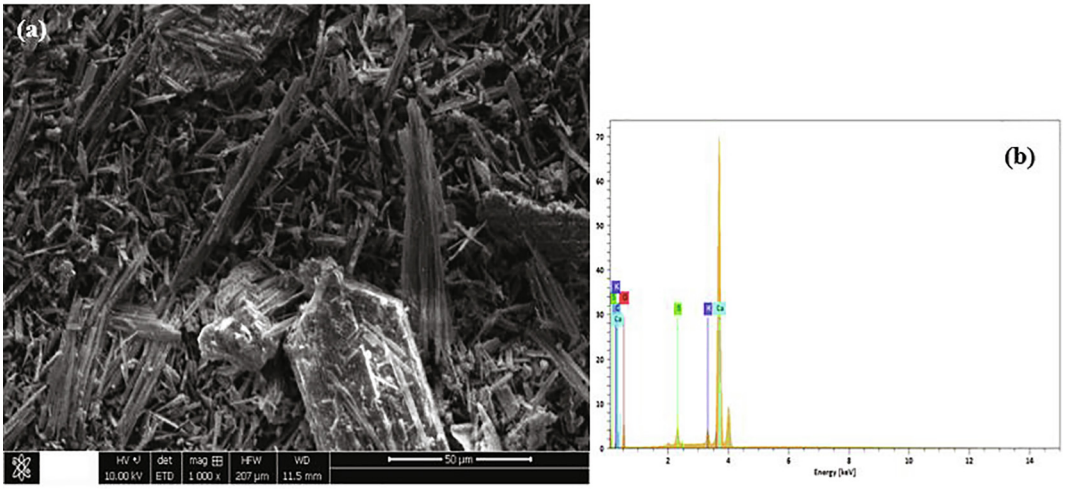

Fig. 8. SEM-EDS analysis of Portlandite $Ca(OH)_2$.

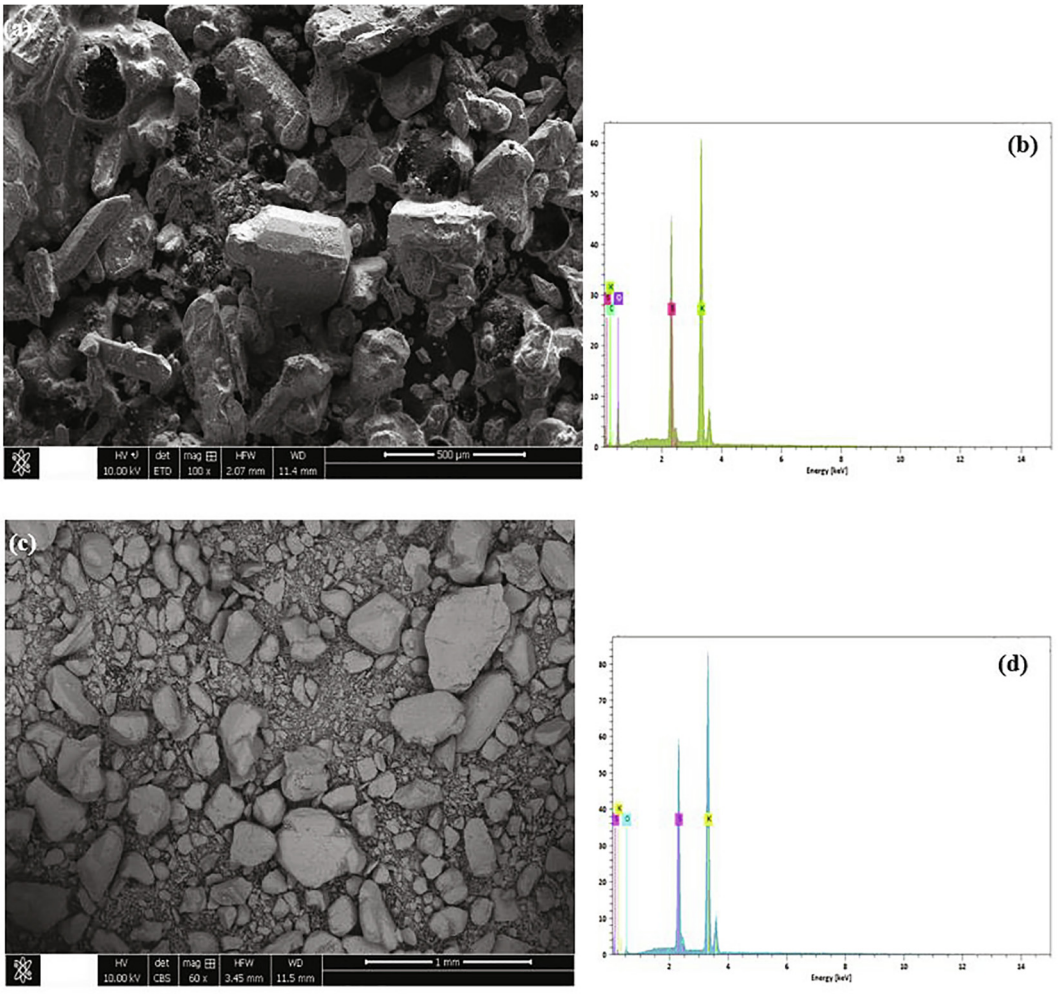

Fig.9. SEM-EDS analysis of (a)-(b) the synthetic, and (c)-(d) the commercial potassium sulphate K_2SO_4.

specific reaction occurs at specific temperatures while the sample is being heated. Furthermore, the TG-DTA curves of the $CaCO_3$ produced at 550–800 °C are very similar to the commercial $CaCO_3$ as shown in Fig. 11b.

For examining the amount carbonation of the product ($CaCO_3$), a CO_2 capture efficiency was determined. To have a general overview on the efficiency of carbonation, a kinetics of the reaction has been presented in Fig. 12 and it showed that

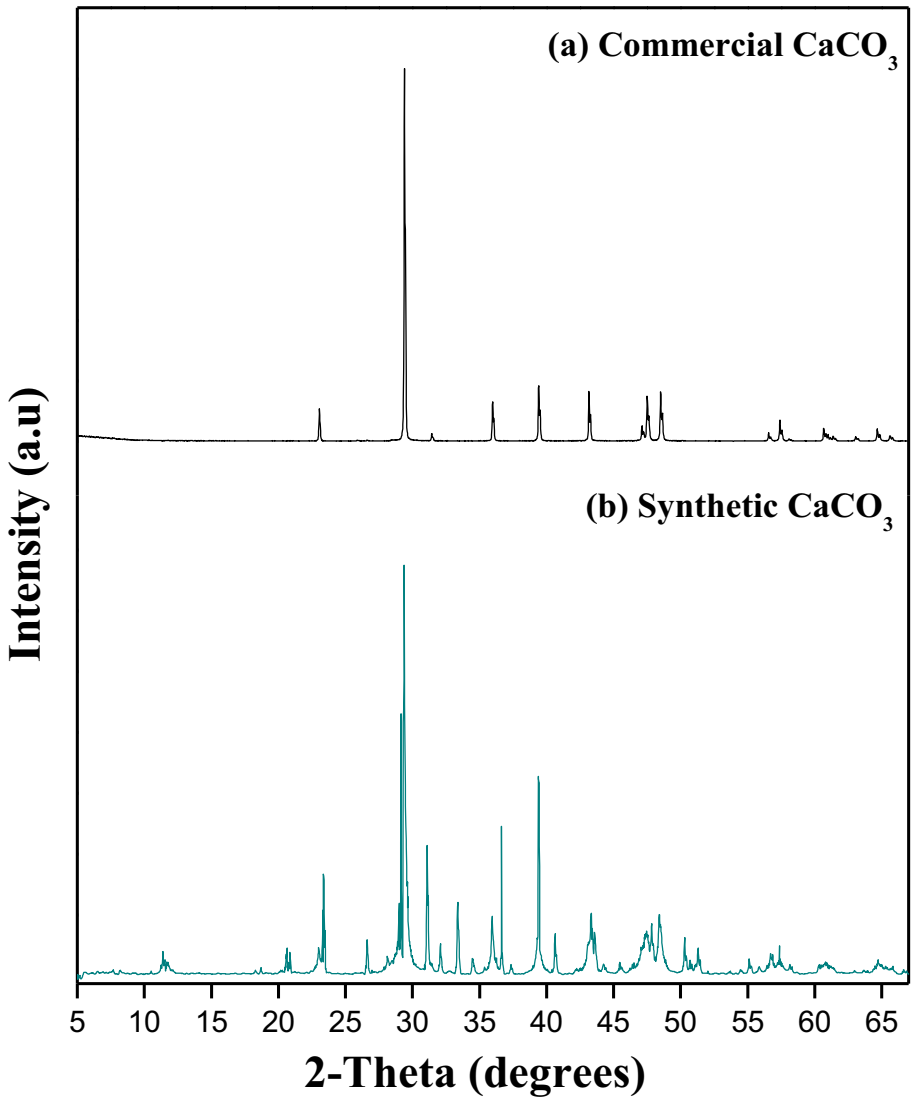

Fig. 10. XRD analysis of (a) commercial and (b) the synthetic calcium carbonate $CaCO_3$.

the carbonation of portlandite is a fast process (reaction time about 15 min).

The carbonation efficiency (C_E) is defined as the ratio between the amount of carbonate formed in the carbonation process (X_{exp}) and the theoretical amount of carbonate (X_{theo}), which possibly formed from the total Ca contained in the phosphogypsum. In General, the capture efficiency is expressed as follows:

$$C_E(\%) = \left(\frac{X_{exp}}{X_{theo}}\right) * 100 \quad (5)$$

The XRF results of phosphogypsum were used to determine the theoretical amount of X_{CO3} formed ($CaCO_3$), which depends on the concentration of calcium Ca contained in the sample. Furthermore, to determine the $CaCO_3$ formed, the TGA results of the carbonation product was used, while the amount of $CaCO_3$ formed in the carbonation method is a function of weight loss, corresponding to the molecule of CO_2, depending on the decomposition Eq. (4) [42]. So, the $CaCO_3$ purity measurement were performed using Eq. (6), in these equation, P stands for product purity, ΔW is the sample weight loss from TGA, and Mw shows molecular weights. In our case, the carbonation efficiency was about 89.86%, and the $CaCO_3$ purity was 72.72%.

$$P_{CaCO3} = \frac{\Delta W(\%) * Mw_{CaCO3}}{Mw_{CO2}} * 100 \quad (6)$$

Fig. 11 represents the FTIR spectrums of the $CaCO_3$ synthetic from carbonation process and the commercial. The peaks observed at 1459.31 cm^{-1}, 869.69 cm^{-1} and 709.25 cm^{-1} correspond to the different vibration modes of carbonates (Fig. 10a). The absorption band around

1459.31 cm^{-1} shows the presence of a strong band correspond to the C—O stretching mode of carbonate with a narrow band at 869.69 cm^{-1} of the bending mode [60,61]. The sharp peak at 709.25 cm^{-1} is assigned to Ca—O bonds. The stretching vibrations of the H_2O molecules in the calcium carbonate occur at 1621.52 cm^{-1} and 3409.60 cm^{-1}. The observed bands at 1134.90 cm^{-1} and 672.89 cm^{-1} corresponding to the sulphate as seen in the phosphogypsum spectrum and as confirmed by the XRD analyses, the strong band at 1134.90 cm^{-1} and the weak band

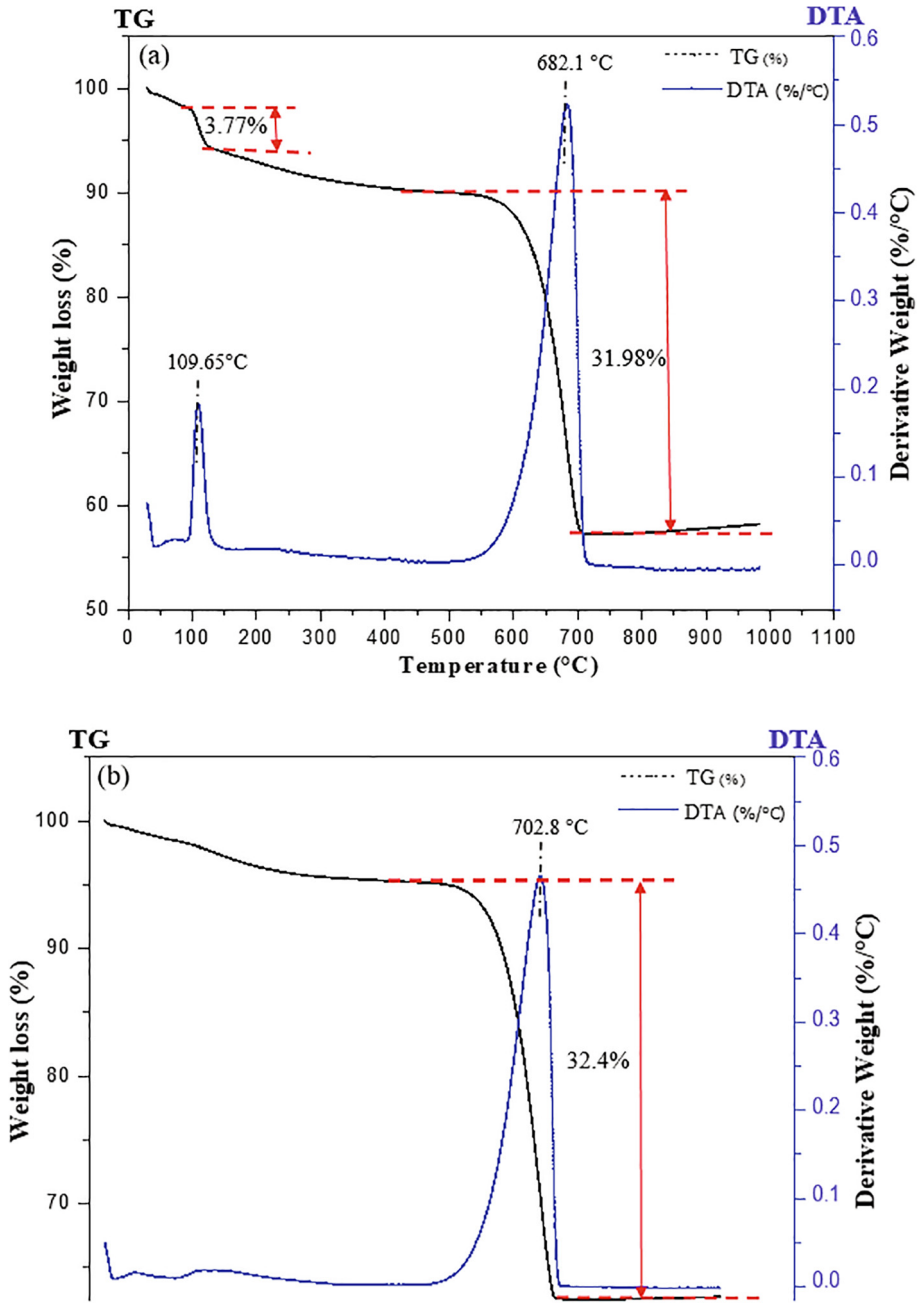

Fig. 11. TG-DTA curves of (a) the synthetic, and (b) the Commercial calcium carbonate $CaCO_3$.

at 672.89 cm^{-1} are related to symmetric and asymmetric S—O bonds. This study confirms that the peaks observed in the sample of $CaCO_3$ produced was very similar to the commercial one Fig. 13b.

In the majority of published works related to the carbonation processes, calcium ions in phosphogypsum can be handily transformed into calcite and vaterite. Hence, phosphogypsum can be supposed as a potential and attractive feedstock for CO_2 sequestration.

Fig. 14a and c presents the SEM-EDS images of the synthetic and the commercial calcium carbonate ($CaCO_3$) after carbonation process. As shown in the Fig. 14a, the particles with rhomboidal and spherical shapes are widely displayed, which confirms the presence of calcite and vaterite in the final product of the carbonation process with variable sizes. The major composed of the carbonation products is the calcite, most of which possess obvious rhombohedral structure as shown in the image, which confirms the high purity of $CaCO_3$. Similar morphology has been previously revealed for calcium carbonate [19,42] and these results are consistent with the commercial $CaCO_3$ and the XRD experiments. Furthermore, this is confirmed by the EDS studies, as shown in Fig. 14b where it can be seen that is mainly composed of Ca (41.26 wt%), C (14.54 wt%) and O (65.29 wt%).

Fig. 14b depicts the typical EDS spectrum of synthesized calcium carbonate. As observed, the EDS spectrum shows peaks for Ca (41.26 wt%), C (14.54 wt%) and O (65.29 wt%) which confirmed that is mainly composed of $CaCO_3$, as indicate in XRF analysis.

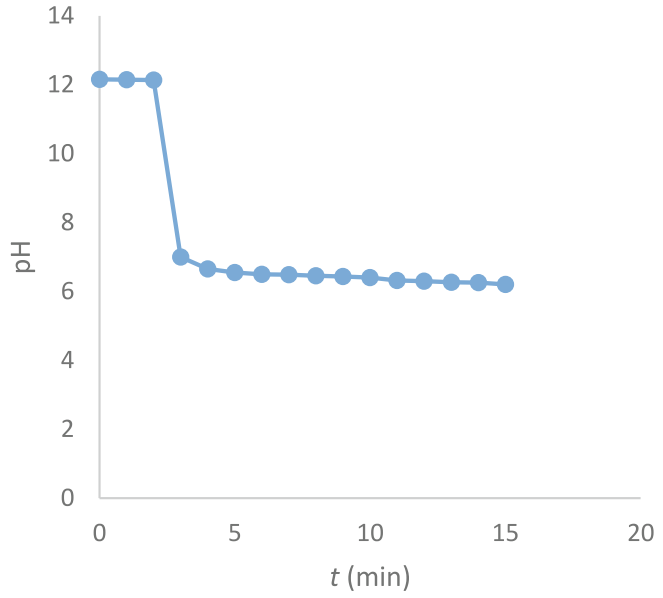

Fig. 12. Kinetics of carbonation of calcium hydroxide obtained by treatment alkaline. phosphogypsum with potassium hydroxide.

Finally, the results of this study confirms that the process applied in this study has several advantages, such as reduction in cost for CO_2 sequestration through the valorization of phosphogypsum waste following by the production of calcium carbonate and release of potassium sulphate as a stable material.

4. Conclusion

The using of secondary product such as phosphogypsum in the industrial sector has achieved a great attention. However, the valorization routes consume about 15% of phosphogypsum amounts; therefore, the demand of this waste is limited and cannot satisfy the quantities produced. In this context, the most promising applications are found in CO_2 sequestration [63] where we can use larger amounts of this by-product.

In this study, the carbon dioxide sequestration was done using an industrial by-product phosphogypsum, due to the large amount of Ca. Their capacity for the storage of CO_2 and their ability to form $CaCO_3$ as a stable compound was evaluated.

To sum up we can say that this method could be considering as a green and sustainable one for reducing CO_2 emissions in large-scale at ambient temperature and atmospheric pressure noting that their efficiency could attempt the rate of 89.86%.

According to the results, the composition of the carbonation product is principally $CaCO_3$ and, the co-product resulting from dispersion of di-hydrated calcium sulphate from the phosphogypsum into potassium hydroxide was potassium sulphate, as expected. Whereas, the results show that the most amounts of impurities are transferred into the calcium carbonate and some of them to potassium sulphate. So, it has been shown that the phosphogypsum as carbonation feedstock is safe and cost effective method to add value to the high amount of this industrial by-product produced by the fertilizer industry and to investigate into the mitigation of the CO_2 emissions. The products obtained $CaCO_3$ and K_2SO_4 with high purity from dispersion and carbonation of the phosphogypsum could be able to be used in different fields such as raw material construction or in agriculture sector.

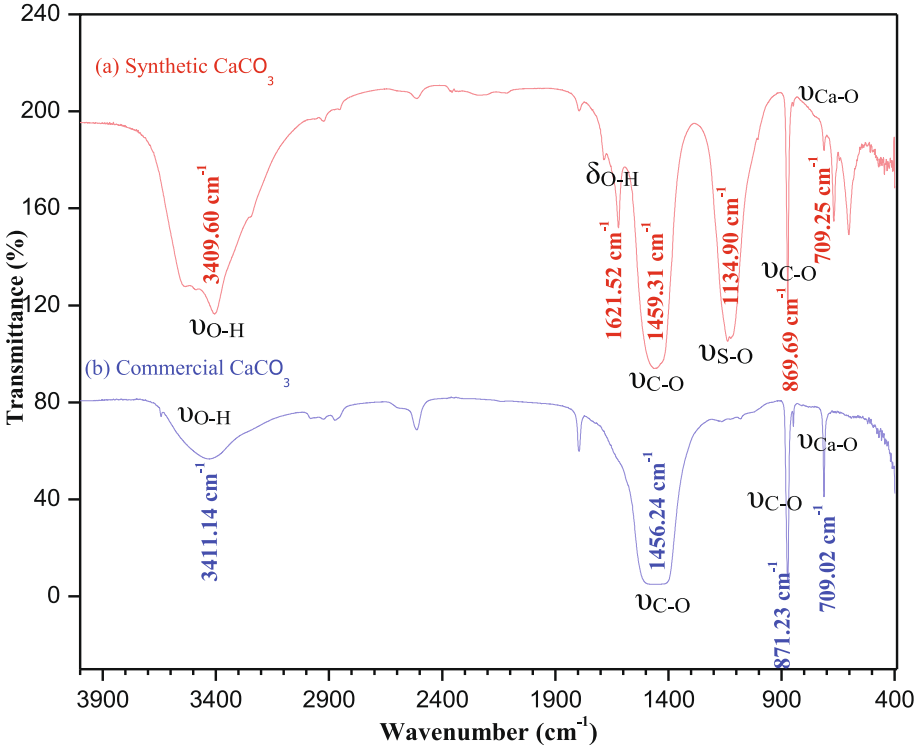

Fig. 13. FTIR analysis of (a) the synthetic, and (b) the commercial calcium carbonate $CaCO_3$.

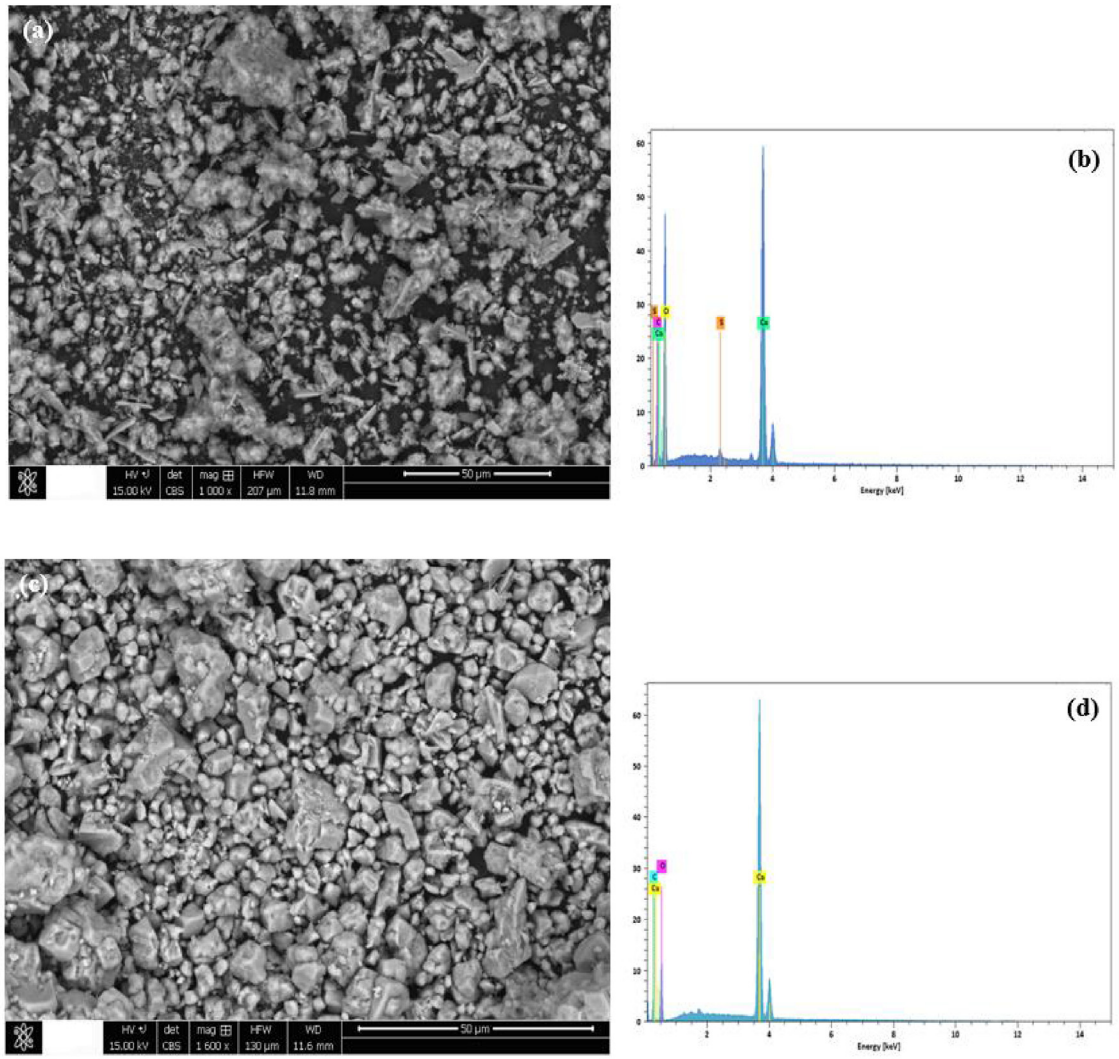

Fig. 14. SEM-EDS analysis of (a)-(b) the synthetic, and (c)-(d) the commercial calcium carbonate $CaCO_3$.

The novel approach presented in this work is to minimize the emissions of CO_2, which causes a serious problems for the ecosystems and human health and to develop a new way to synthesis potassium sulphate by using the co-product phosphogypsum coming from fertilizer industry.

CRediT authorship contribution statement

Adil Lachehab: Conceptualization, Funding Acquisition, Methodology, Writing - original draft, Investigation, Visualization Resources. **Oumaima Mertah:** Investigation. **Abdelhak Kherbeche:** Resources. **Hicham Hassoune:** Conceptualization; Supervision; Validation; Methodology; Writing - original draft; Visualization; Funding Acquisition; Writing – Review & Editing; Resources.

Declaration of Competing Interest

The authors declare that they have no known competing financial interests or personal relationships that could have appeared to influence the work reported in this paper.

References

[1] B. Metz, O. de Davidson, H.C. Coninck, M. Loos, L.J. Meyer (Eds.), IPCC: Special Report on Carbon Dioxide Capture and Storage, Cambridge University Press, Cambridge, UK, 2005.
[2] R. Farajzadeh, P.L.J. Zitha, J. Bruining, Enhanced mass transfer of CO_2 into water: experiment and modeling, Ind. Eng. Chem. Res. 48 (2009) 6423–6643, https://doi.org/10.1021/ie801521u.
[3] B. Metz, O. Davidson, R. Swart, J. Pan (Eds.), IPCC: The Third Assessment Report of the Intergovernmental Panel on Climate Change-Mitigation, Cambridge University Press, Cambridge, UK, 2001, https://doi.org/10.1177/095968360301300516.
[4] K. Mosher, J. He, Y. Liu, E. Rupp, J. Wilcox, Molecular simulation of methane adsorption in micro-and mesoporous carbons with applications to coal and gas shale systems, Int. J. Coal Geol. 109 (2013) 36–44, https://doi.org/10.1016/j.coal.2013.01.001.
[5] S.J. Davis, K. Caldeira, H.D. Matthews, Future CO_2 emissions and climate change from existing energy infrastructure, Science 329 (2010) 1330–1333, https://doi.org/10.1126/science.1188566.
[6] M.I. Hoffert, K. Caldeira, G. Benford, D.R. Criswell, C. Green, H. Herzog, A.K. Jain, H.S. Kheshgi, K.S. Lackner, J.S. Lewis, H.D. Lightfoot, W. Manheimer, J.C. Mankins, M.E. Mauel, L.J. Perkins, M.E. Schlesinger, T. Volk, T.M.L. Wigley, Advanced technology paths to global climate stability: energy for a greenhouse planet, Science 298 (2002) 981–987, https://doi.org/10.1126/science.1072357.
[7] G. Gadikota, J. Matter, P. Kelemen, H.A. Park, Chemical and morphological changes during olivine carbonation for CO_2 storage in the presence of NaCl and $NaHCO_3$, Phys. Chem. 16 (2014) 4679–4693, https://doi.org/10.1039/c3cp54903h.

[8] P. Goodwin, A. Katavouta, V.M. Roussenov, G.L. Foster, E.J. Rohling, R.G. Williams, Pathways to 1.5 and 2 °C warming based on observational and geological constraints, Nat. Geosci. 11 (2018) 1–22, https://doi.org/10.1038/s41561-017-0054-8.

[9] P.H. Israelsson, A.C. Chow, E.E. Adams, An updated assessment of the acute impacts of ocean carbon sequestration by direct injection, Energy Procedia 1 (2009) 4929–4936, https://doi.org/10.1016/j.egypro.2009.02.324.

[10] D.X. Zhang, J. Song, Mechanisms for geological carbon sequestration, Proc. Iutam. 10 (2014) 319–327, https://doi.org/10.1016/j.piutam.2014.01.027.

[11] H. Zhao, H. Li, W. Bao, C. Wang, S. Li, W. Lin, Experimental study of enhanced phosphogypsum carbonation with ammonia under increased CO_2 pressure, J. CO_2 Util. 11 (2015) 10–19, https://doi.org/10.1016/j.jcou.2014.11.004.

[12] J.M. Matter, P.B. Kelemen, Permanent storage of carbon dioxide in geological reservoirs by mineral carbonation, Nat. Geosci. 2 (2009) 837–841, https://doi.org/10.1038/ngeo683.

[13] O. Rahmani, CO_2 sequestration by indirect mineral carbonation of industrial waste red gypsum, J. CO_2 Util. 27 (2018) 374–380, https://doi.org/10.1016/j.jcou.2018.08.017.

[14] A.A. Olajire, Review of mineral carbonation technology in sequestration of CO_2, J. Petrol. Sci. Eng. 109 (2013) 364–392, https://doi.org/10.1016/j.petrol.2013.03.013.

[15] K.S. Lackner, Carbonate chemistry for sequestering fossil carbon, Ann. Rev. Enegy Environ. 27 (2002) 193–232, https://doi.org/10.1146/annurev.27.122001.083433.

[16] S. Tian, J. Jiang, Sequestration of flue gas CO_2 by direct gas-solid carbonation of air pollution control system residues, Environ. Sci. Technol. 46 (2012) 13545–13551, https://doi.org/10.1021/es303713a.

[17] A. Sanna, K. Wang, A. Lacinska, M. Styles, T. Paulson, M.M. Maroto-Valer, Enhancing Mg extraction from lizardite-rich serpentine for CO_2 mineral sequestration, Min. Eng. 49 (2013) 135–144, https://doi.org/10.1016/j.mineng.2013.05.018.

[18] W.J.J. Huijgen, G.J. Witkamp, R.N.J. Comans, Mechanisms of aqueous wollastonite carbonation as a possible CO_2 sequestration process, Chem. Eng. Sci. 61 (2006) 4242–4251, https://doi.org/10.1016/j.ces.2006.01.048.

[19] A. Azdarpour, M. Asadullah, R. Junin, A. Manan, H. Hamidi, M. Erfan, Direct carbonation of red gypsum to produce solid carbonates, Fuel. Proces. Technol. 126 (2014) 429–434, https://doi.org/10.1016/j.fuproc.2014.05.028.

[20] F. Wang, D. Dreisinger, M. Jarvis, T. Hitchins, Kinetics and mechanism of mineral carbonation of olivine for CO_2 Sequestration, Min. Eng. 131 (2019) 185–197, https://doi.org/10.1016/j.mineng.2018.11.024.

[21] I.S. Romão, M.G.-F. Licinio, V.G. Silva, R. Zevenhoven, CO_2 sequestration with serpentinite and metaperidotite from Northeast Portugal, Min. .Eng. 94 (2016) 104–114, https://doi.org/10.1016/j.mineng.2016.05.009.

[22] K.W. Ryu, M.G. Lee, Y.N. Jang, Mechanism of tremolite carbonation, Appl. Geochem. 2011 (26) (2011) 1215–1221, https://doi.org/10.1016/j.apgeochem.2011.04.010.

[23] S. Eloneva, S. Teir, J. Salminen, C.-J. Fogelholm, R. Zevenhoven, Fixation of CO_2 by carbonation calcium derived from blast furnace slag, Energy J. 33 (2008) 1461–1467, https://doi.org/10.1016/j.energy.2008.05.003.

[24] A. Iizuka, M. Fujii, A. Yamasaki, Y. Yanagisawa, Development of a new CO_2 sequestration process utilizing the carbonation of waste cement, Ind. Eng. Chem. Res. 43 (2004) 7880–7887, https://doi.org/10.1021/ie0496176.

[25] P.M. Rutherford, M.J. Dudas, R.A. Samek, Environmental impacts of phosphogypsum, Sci. Total Environ. 149 (1994) 1–38, https://doi.org/10.1016/0048-9697(94)90002-7.

[26] F. Habashi, The recovery of the lanthanides from phosphate rock, J. Chem. Technol. Biotechnol. 35 (1985) 5–14, https://doi.org/10.1002/jctb.5040350103.

[27] S. Zhao, L. Ma, J. Yang, D. Zheng, H. Liu, J. Yang, Mechanism of CO_2 capture technology based on the phosphogypsum reduction thermal decomposition process, Energy Fuels 31 (2017) 9824–9832, https://doi.org/10.1021/acs.energyfuels.7b01673.

[28] L. Reijnders, Cleaner phosphogypsum, coal combustion ashes and waste incineration ashes for application in building materials: a review, Build. Environ. 42 (2007) 1036–1042, https://doi.org/10.1016/j.buildenv.2005.09.016.

[29] H. Tayibi, M. Choura, F.A. López, F.J. Alguacil, A. López-Delgado, Environmental impact and management of phosphogypsum, J. Environ. Manage. 90 (2009) 2377–2386, https://doi.org/10.1016/j.jenvman.2009.03.007.

[30] C. Dueñas, E. Liger, S. Cañété, M. Pérez, J.P. Bolívar, Exhalation of ^{222}Rn from phosphogypsum piles located at the Southwest of Spain, J. Environ. Radioact. 95 (2007) 63–74, https://doi.org/10.1016/j.jenvrad.2007.01.012.

[31] I. Fauziah, S. Zauyah, T. Jamal, Characterization and land application of RG: a waste product from the titanium dioxide industry, Sci. Total Environ. 188 (1996) 243–251, https://doi.org/10.1016/0048-9697(96)05179-0.

[32] M.J. Gazquez, J.P. Bolivar, F. Vaca, R. García-Tenorio, A. Caparros, Evaluation of the use of TiO_2 industry RG waste in cement production, Cem. Concr. Compos. 37 (2013) 76–81, https://doi.org/10.1016/j.cemconcomp.2012.12.003.

[33] N. Mechi, R. Khiari, M. Ammar, E. Elaloui, M.N. Belgacem, Preparation and application of Tunisian phosphogypsum as fillers in papermaking made from Prunus amygdalus and Tamarisk sp., Powder Technol. 312 (2017) 287–293, https://doi.org/10.1016/j.powtec.2017.02.055.

[34] S.M. Pérez-Moreno, M.J. Gázquez, A.G. Barneto, J.P. Bolívar, Thermal characterization of new fire-insulating materials from industrial inorganic TiO_2 wastes, Thermochim. Acta 552 (2013) 114–122, https://doi.org/10.1016/j.tca.2012.10.021.

[35] L. Ajam, M.B. Ouezdou, H.S. Felfoul, R. El Mensi, Characterization of the Tunisian phosphogypsum and its valorization in clay bricks, Constr. Build. Mater. 25 (2009) 3240–3247, https://doi.org/10.1016/j.conbuildmat.2009.05.009.

[36] Q. Zhao, C.J. Liu, M.F. Jiang, H. Saxén, R. Zevenhoven, Preparation of magnesium hydroxide from serpentinite by sulfuric acid leaching for CO_2 mineral carbonation, Min. Eng. 79 (2015) 116–124, https://doi.org/10.1016/j.mineng.2015.06.002.

[37] C. Cárdenas-Escudero, V. Morales-Flórez, R. Pérez- López, A. Santos, L. Esquivias, Procedure to use phosphogypsum industrial waste for mineral CO_2 sequestration, J. Hazard. Mater. 196 (2011) 431–435, https://doi.org/10.1016/j.jhazmat.2011.09.039.

[38] H. Xie, J. Wang, Z. Hou, Y. Wang, T. Liu, L. Tang, W. Jiang, CO_2 sequestration through mineral carbonation of waste phosphogypsum using the technique of membrane electrolysis, Environ. Earth. Sci. 75 (2016) 1216, https://doi.org/10.1007/s12665-016-6009-3.

[39] Y. Dong, X. Bian, Y. Fu, Q. Shao, J. Jiang, Simple preparation of potassium sulfate nanoparticles, Cryst. Eng. Comm. 20 (2018) 7713–7718, https://doi.org/10.1039/c8ce01373j.

[40] L. Esquivias, V. Morales-Flórez, A. Santos, Carbon dioxide sequestration by phosphogypsum based procedure, in: F. Pacheco-Torgal, C. Shi, A.P. Sanchez (Eds.), Carbon Dioxide Sequestration in Cementitious Construction Materials, Woodhead Publishing, Duxford, 2018, pp. 199–223, https://doi.org/10.1016/B978-0-08-102444-7.00009-5.

[41] S.I. Abu-Eishah, A.A. Bani-Kananeh, M.A. Allawzi, K_2SO_4 production via the double decomposition reaction of KCl and phosphogypsum, Chem. Eng. J. 76 (2000) 197–207, https://doi.org/10.1016/S1385-8947(99)00158-8.

[42] R.L. Rudnick, S. Gao, Composition of the continental crust, Treat. Geochem. 3 (2003) 1–64, https://doi.org/10.1016/B0-08-043751-6/03016-4.

[43] S.M. Pérez-Moreno, M.J. Gázquez, A.G. Barneto, J.P. Bolívar, CO_2 seqestration by indirect carbonation of artificial gypsum generated in the manufacture of titanium dioxide pigments, Chem. Eng. J. 262 (2015) 737–746, https://doi.org/10.1016/j.cej.2014.10.023.

[44] S.M. Luther, M.J. Dudas, P.M. Rutherford, Radioactivity and chemical characteristics of alberta phosphogypsum, Water Air Soil Pollut. 69 (1993) 277–290, https://doi.org/10.1007/BF00478164.

[45] I. Hammas, K.N. Horchani, M. Férid, Solubility study and valorization of phosphogypsum salt solution, Int. J. Miner. Process. 123 (2013) 87–93, https://doi.org/10.1016/j.minpro.2013.02.008.

[46] G. Socrates, Infrared and Raman characteristic group frequencies, third ed. John Wiley, New York, 2001. https://dx.doi.org/10.1002/jrs.1238.

[47] I. Hammas, N.K. Karima Horchani, M. Férid, D. Barca, Rare earths concentration from phosphogypsum waste by two-step leaching method, Int. J. Miner. Process. 149 (2016) 78–83, https://doi.org/10.1016/j.minpro.2016.02.011.

[48] H. Böke, S. Akkurtb, S. Özdemirb, H.E. Gökturkc, C.N.E. Saltik, Quantification of $CaCO_3$-$CaSO_3 0.5H_2O$–$CaSO_4$-$2H_2O$ mixtures by FTIR analysis and its ANN model, Mater. Lett. 58 (2004) 723–726, https://doi.org/10.1016/j.matlet.2003.07.008.

[49] M.B. Kruger, Q. Williams, R. Jeanloz, Vibrational spectra of $Mg(OH)_2$ and $Ca(OH)_2$ under pressure, J. Chem. Phys. 91 (1989) 5910, https://doi.org/10.1063/1.457460.

[50] E.T. Stepkowska, Hypothetical transformation of $Ca(OH)_2$ into $CaCO_3$ in solid-state reactions of Portland cement, J. Therm. Anal. Cal. 80 (2005) 727–733, https://doi.org/10.1007/s10973-005-0721-7.

[51] E.E. Fenn, M.D. Fayer, Water hydrogen bonding dynamics at charged interfaces observed with ultrafast nonlinear vibrational spectroscopy, in: A. Wieckowski, C. Korzeniewski, B. Braunschweig (Eds.), Vibrational Spectroscopy at Electrified Interfaces, Wiley, 2013, pp. 1–47, https://doi.org/10.1002/978118658871.ch1.

[52] E.S. Park, H.W. Ro, C.V. Nguyen, R.L. Jaffe, D.Y. Yoon, Infrared Spectroscopy Study of Microstructures of Poly(silsesquioxane)s, Chem. Mater. 20 (2007) 1548–1554, https://doi.org/10.1021/cm071575z.

[53] S.C.B. Myneni, J.S. Traina, A.G. Waychunas, T.J. Logan, Vibrational spectroscopy of functional group chemistry and arsenate coordination in ettringite, Geochim. Cosmochim. Acta. 62 (1998) 3499–3514, https://doi.org/10.1016/S0016-7037(98)00221-X.

[54] M.R. Querry, R.C. Waring, W.E. Holland, L.M. Earls, M.D. Herrman, W.P. Nijm, G. M. Hale, Optical-Constants in Infrared for K_2SO_4, $NH_4H_2PO_4$, and H_2SO_4 in Water, J. Opt. Soc. Am. 64 (1974) 39–46, https://doi.org/10.1364/JOSA.64.000039.

[55] A. Lachehab, A. Kherbeche, B. El Bali, H. Hassoune, CO_2 Mineral sequestration by using phosphogypsum as adsorbent, Eur. J. Sci. Res. 143 (2017) 366–376.

[56] V.M. Rentería, I. Vioque, J. Mantero, G. Manjón, Radiological, chemical and morphological characterizations of phosphate rock and phosphogypsum from phosphoric acid factories in SW Spain, J. Hazard. Mater. 181 (2010) 193–203, https://doi.org/10.1016/j.jhazmat.2010.04.116.

[57] K. Grabas, A. Adam Pawełczyk, W. Stręk, E. Eligiusz Szełęg, S. Stręk, Study on the properties of waste apatite phosphogypsum as a raw material of prospective applications, Waste. Biomass. Valori. (2018), https://doi.org/10.1007/s12649-018-0316-8.

[58] K. Kuryatnyk, C. Angulski da Luz, J. Ambroise, Valorization of phosphogypsum as hydraulic binder, J. Hazard. Mater. 160 (2008) 681–687, https://doi.org/10.1016/j.jhazmat.2008.0.014.

[59] Q. Xu, G.T. Rochelle, Solvent reclaiming by crystallization of potassium sulfate, Energy Procedia 1 (2009) 1205–1212, https://doi.org/10.1016/j.egypro.2009.01.158.

[60] J.P. Sanders, P.K. Gallagher, Kinetic analyses using simultaneous TG/DSC measurements. Part I. Decomposition of calcium carbonate in argon, Thermochim. Acta 388 (2002) 115–128, https://doi.org/10.1016/S0040-6031(02)00032-1.

[61] R.M. Galván, J. Hernández, L. Baños, M.N. Joaquín, G.M.E. Rodríguez, Characterization of calcium carbonate, calcium oxide, and calcium hydroxide as starting point to the improvement of lime for their use in construction, J. Mater. Civ. Eng. 21 (2009) 625–708, https://doi.org/10.1061/(ASCE)0899-1561(2009)21:11(694).

[62] S. Takahama, G. Ruggeri, M.A. Dillner, Analysis of functional groups in atmospheric aerosols by infrared spectroscopy: sparse methods for statistical selection of relevant absorption bands, Atmospheric. Meas. Technol. 9 (2016) 3429–3454, https://doi.org/10.5194/amt-9-3429-2016.

[63] E. Ruiz, K. Kudłacz, V. Putnis, A. Putnis, C. Rodriguez, Dissolution and carbonation of Portlandite [$Ca(OH_)2$] single crystals, Environ. Sci. Technol. 47 (2013) 11342–11349, https://doi.org/10.1021/es402061c.